Karcher Mean in Elastic Shape Analysis

Wen Huang[1], Yaqing You[2] K. A. Gallivan[2], P.-A. Absil[1]

[1]Université catholique de Louvain, [2]Florida State University

This paper presents research results of the Belgian Network DYSCO (Dynamical Systems, Control, and Optimization), funded by the Interuniversity Attraction Poles Programme initiated by the Belgian Science Policy Office. This work was supported by grant FNRS PDR T.0173.13.

Introduction

Shape analysis of curves is important in various area such as computer vision, medical diagnostics, and bioinformatics. The basic idea is to obtain a boundary curve of an object in a 2D image or contours of a 3D object and analyse those curves to characterize the original object. Elastic shape analysis is receiving increasing attention due to its superior theoretical results and effectiveness. The price for the improved effectiveness is the relative increase in expense in computing various objects, e.g., geodesics and means. In this poster, we compare the performance of recent geodesic algorithm in [YHGA15] to the existing geodesic algorithm in [SKJJ11] in computing Karcher mean.

Elastic Shape Analysis

Inelastic shape analysis invariants: (i) **Rescaling** (ii) **Translation** (iii) **Rotation**. Elastic shape analysis additional invariant: (vi) **Reparametrization**.

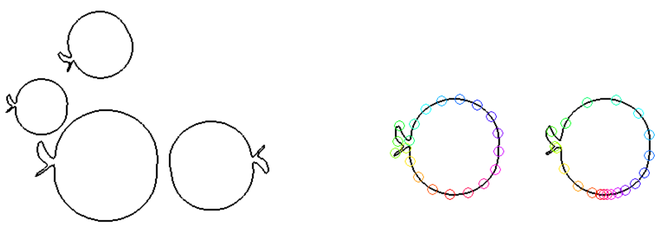

Figure 1: All are the same shape.

Elastic shape analysis has been studied in many papers, e.g., [You98, KSMJ04, YMSM08, SKJJ11].

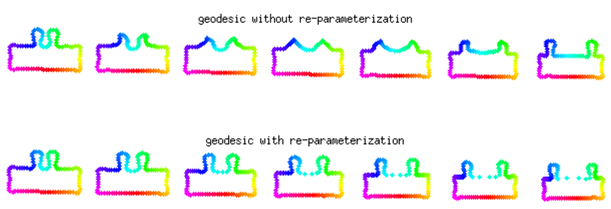

Figure 2: Geodesics without and with reparameterization are given by the frameworks of landmark-based Kendall's shape analysis [Ken84, DM98] and elastic shape analysis [SKJJ11] respectively.

Square Root Velocity

The square root velocity (SRV) framework given in [SKJJ11] for elastic shape analysis of general n dimensional curves is considered.

In this poster, we only consider closed curves $\beta(t) : \mathbb{S}^1 \to \mathbb{R}^n$. Its square root velocity (SRV) function is $q(t) = \frac{\dot\beta(t)}{\sqrt{\|\dot\beta(t)\|}}$, where $\|\cdot\|$ denotes 2-norm.

The preshape space l_n (that removes translation and rescaling) is

$$\left\{ q \in \mathbb{L}^2 | \int_{\mathbb{S}^1} ||q(t)||dt = 1, \int_{\mathbb{S}^1} q(t)||q(t)||dt = 0 \right\}.$$

The shape space $\mathfrak{L}_n$ (that further removes rotation and reparameterization) is

$$l_n/(\Gamma \times \mathrm{SO}(n)) = \{\overline{[q]} | q \in l_n\},$$

where $\overline{[q]}$ denotes the closure of $[q] := \left\{O(q\circ\gamma)\sqrt{\dot\gamma} | (\gamma, O) \in \Gamma \times \mathrm{SO}(n)\right\}$, and $\mathrm{SO}(n)$ and Γ denote the rotation group and the reparameterization group respectively.

Karcher Mean

The Karcher mean of shapes $\overline{[q_i]}, i = 1, 2, \ldots, N$ is defined to be the minimizer of the cost function

$$[q_*] = \arg\min_{[q]\in\mathcal{L}_n} \frac{1}{2N} \sum_{i=1}^{N} \mathrm{d}^2_{\mathcal{L}_n}(\overline{[q]}, \overline{[q_i]}). \quad (1)$$

where

$$\mathrm{d}_{\mathcal{L}_n}(\overline{[q]}, \overline{[q_i]}) = \inf_{(\gamma,O)\in\Gamma\times\mathrm{SO}(n)} \mathrm{d}_{l_n}(q, O(q_i\circ\gamma)\sqrt{\dot\gamma}).$$

A representation of the gradient of (1) is given by $\frac{1}{N}\sum_{i=1}^{N} \dot\alpha_i(1)$, where $\alpha_i \subset l_n$ is the minimum geodesic such that $\alpha_i(1) = q$ and $\alpha_i(0) \in \overline{[q_i]}$. (Numerically, we only guarantee to find a constant velocity geodesic.)

Geodesic Algorithm

The closed form of distance $d_{\mathfrak{L}_n}$ is unknown, hence we compute it with an algorithm sketched in Figure 3.

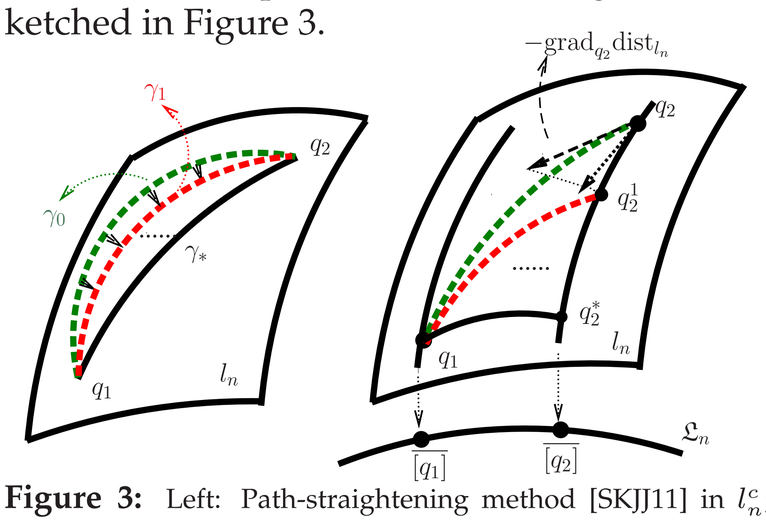

Figure 3: Left: Path-straightening method [SKJJ11] in l_n^c; Right: Remove rotation and reparameterization.

Two approaches for removing rotation and reparameterization (i.e., finding q_2^* in $\overline{[q_2]}$) are used: (i) Coordinate descent method [SKJJ11] (ii): Riemannian quasi-Newton method [YHGA15].

Algorithm

Algorithm 1 Karcher Mean

Input: Curves $\beta_i, i = 1, \ldots, N$ and initial iterate $\beta^{(0)}$.

1: Compute the representations $q^{(0)}$ of $\beta^{(0)}$ and q_i of β_i, $i = 1, \ldots, N$ in l_n. Set $k = 0$.

2: Compute the shortest curve α_i such that $\alpha_i(1) = q^{(k)}$ and $\alpha_i(0) \in \overline{[q_i]}$ for all $i = 1, \ldots, N$. The values of the cost function (1) and its gradient are obtained during this computation.

3: Apply the backtracking line search algorithm [DS83, Algorithm A6.3.1] and find the step size λ_k and the next iterate

$$q^{(k+1)} = R_{q^{(k)}}(-\lambda_k\zeta_k), \quad (2)$$

where $\zeta_k = \frac{1}{N}\sum_{i=1}^{N}\dot\alpha_i(1)$ is the gradient of (1).

4: If some stopping criterion is satisfied, then stop. Else, $k \leftarrow k+1$ and goto Step 2.

Experiments

The MPEG-7 dataset [Uni] is used in the experiments. Algorithm 1 with the approaches in [SKJJ11] and [YHGA15] are denoted by MeanCD and MeanLRBFGS respectively.

Table 1: Computational time, number of iterations and final cost function values of reported tests. t, iter and f denote computational time (second), number of iterations and final cost function value respectively. The subscript k indicates a scale of 10^k.

	MeanCD [SKJJ11]			MeanLRBFGS [YHGA15]		
	t	iter	f	t	iter	f
Figure 4	2.94_2	27	5.03_{-2}	9.87_1	8	4.99_{-2}
Figure 5	7.05_2	26	3.93_{-2}	4.55_2	14	3.67_{-2}
Figure 6	1.46_3	19	1.18_{-1}	6.77_2	8	7.40_{-2}

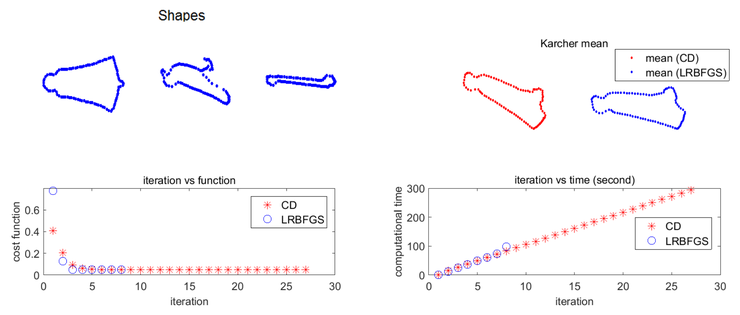

Figure 4: A representative test. The sample shapes and the Karcher means by MeanCD and MeanLRBFGS, cost function values and computational time are given.

Figure 5: A representative test. The sample shapes and the Karcher means by MeanCD and MeanLRBFGS are given.

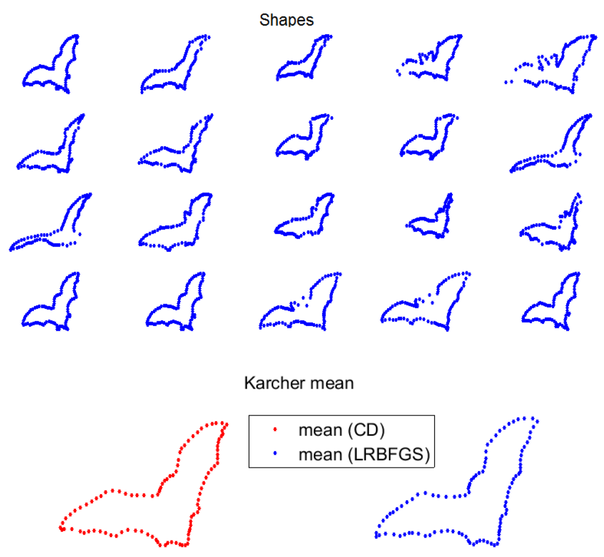

Figure 6: A representative test. The samples shapes, Karcher means by MeanCD and MeanLRBFGS are given.

Conclusion and Future Work

Two approaches for computing elastic shape geodesics required have been given in [SKJJ11] and [YHGA15]. Here we have compared their performance in computing the Karcher mean. We have shown that Algorithm 1 with the approach in [YHGA15] converges faster.

In the future, we will test the quality of the Karcher mean by MeanLRBFGS in the sense of superior clustering, classification and stochastic analysis.

references

[DM98] I. L. Dryden and K. V. Mardia. *Statistical shape analysis*. Wiley, 1998.

[DS83] J. E. Dennis and R. B. Schnabel. *Numerical methods for unconstrained optimization and nonlinear equations*. Springer, New Jersey, 1983.

[Ken84] D. G. Kendall. Shape manifolds, procrustean metrics, and complex projective spaces. *Bulletin of the London Mathematical Society*, 16(2):81–121, March 1984.

[KSMJ04] E. Klassen, A. Srivastava, W. Mio, and S. H. Joshi. Analysis of planar shapes using geodesic paths on shape spaces. *IEEE transactions on pattern analysis and machine intelligence*, 26(3):372–83, March 2004. doi:10.1109/TPAMI.2004.1262333.

[SKJJ11] A. Srivastava, E. Klassen, S. H. Joshi, and I. H. Jermyn. Shape analysis of elastic curves in Euclidean spaces. *IEEE Transactions on Pattern Analysis and Machine Intelligence*, 33(7):1415–1428, September 2011. doi:10.1109/TPAMI.2010.184.

[Uni] Temple University. Shape similarity research project. www.dabi.temple.edu/ shape/MPEG7/dataset.html.

[YHGA15] Y. You, W. Huang, K. A. Gallivan, and P.-A. Absil. A Riemannian Approach for Computing Geodesics in Elastic Shape Analysis. *In Proceedings of the 3rd IEEE Global Conference on Signal and Information Processing, Accepted*, 2015.

[YMSM08] L. Younes, P. Michor, J. Shah, and D. Mumford. A metric on shape space with explicit geodesics. *Rendiconti Lincei - Matematica e Applicazioni*, 9(1):25–57, 2008. doi:10.4171/RLM/506.

[You98] L. Younes. Computable elastic distances between shapes. *SIAM Journal on Applied Mathematics*, 58(2):565–586, April 1998. doi:10.1137/S0036139995287685.